Microwave controlled ground state coherence in an atom-based optical amplifier

K V Adwaith, K N Pradosh, J K Saaswath, Fabien Bretenaker, Andal Narayanan

Research Article Vol. 4, No. 2 / 15 February 2021 / OSA Continuum 702

Microwave controlled ground state coherence in an atom-based optical amplifier

K. V. ADWAITH,[1,3] K. N. PRADOSH,[1] J. K. SAASWATH,[1] FABIEN BRETENAKER,[1,2] AND ANDAL NARAYANAN[1,4]

[1]*Light and Matter Physics Group, Raman Research Institute, Bangalore 560080, India*
[2]*Université Paris-Saclay, CNRS, ENS Paris-Saclay, CentraleSupélec, LuMIn, 91190 Gif-sur-Yvette, France*
[3]*adwaith@rri.res.in*
[4]*andal@rri.res.in*

Abstract: We experimentally investigate and theoretically analyze the effect of microwave controlled atomic ground state coherence on the phase-dependent amplification (PDA) of an optical probe field. We use three hyperfine levels in room temperature ^{85}Rb atoms, which are cyclically connected by two optical and one microwave electromagnetic field. We show that a simultaneous fulfilment of a two-photon resonance condition that creates ground state coherence and a three-photon resonance condition leads to a significantly higher amplification of 7.5 dB of the optical probe field with a visibility of 98.8 %. By selectively breaking the ground state coherence using microwaves, we show that the amplification reduces with a bandwidth of 5 MHz. Nevertheless, the system shows non-zero PDA for large two-photon detunings of 15 MHz with high visibility of 66.8 %. This novel, controllable hybrid-PDA can be potentially used to trade-off amplification for bandwidth during the transmission of phase coherent classical and quantum information.

1. Introduction

Atom-based sensors and radio-over-fibre atomic antennas are rapidly emerging as preferred architectures for sensing platforms and signal communication between microwave and optical frequencies [1–3]. Advances in quantum electrodynamical superconducting circuits operating in the microwave domain for quantum information processing, has stimulated strong interest in developing interfaces between these two frequencies [4,5]. In this context hybrid-amplifiers which will enable coherent conversion and amplification of signals between microwave and optical frequencies play a crucial role.

In traditional nonlinear optics, amplification of a probe field saturates due to linear and nonlinear absorption, especially near atomic resonances [6]. Experimental realization of electromagnetically induced transparency(EIT) [7,8] and coherent population trapping (CPT) [9–11] eliminates linear absorption by a large fraction, thereby enabling nonlinear amplification close to resonance. This opened the new field of low light intensity nonlinear optics. The physical effect of CPT in inducing a ground state coherence through the formation of dark state is at the heart of elimination of linear response [12] and modification of nonlinear responses in atomic media [13]. There have been demonstrations of nonlinear wave mixing and optical amplification using resonant atomic systems [14–17] which exploit this ground state coherence. However, no thorough investigation of ground state coherence linked to two-photon mechanisms and their effect on three-photon processes has been experimentally performed.

In this letter, we present experimental results of an atomic PDA whose ground state coherence is controlled using microwaves and the amplification is observed at optical frequencies. We have used a three-level atomic configuration in room temperature ^{85}Rb atoms to achieve the amplification. These three levels are connected cyclically by two optical fields and one microwave field rendering a closed, cyclic interaction of atomic dipoles with all the three electromagnetic

#413297 https://doi.org/10.1364/OSAC.413297
Journal © 2021 Received 26 Oct 2020; revised 26 Jan 2021; accepted 26 Jan 2021; published 4 Feb 2021

OSA CONTINUUM

fields. This closed system is sensitive to the relative phase of all the three fields, thus making the output probe intensity dependent on the relative phase between all the three fields.

In our earlier work [18], phase dependent amplification (PDA) of the probe field was seen using this system. In the present study, we investigate the explicit role of ground state coherence in our probe transmission by selectively breaking the two-photon resonance, which creates ground state coherence. We, therefore for the first time, experimentally quantify the role of ground state coherence in a phase dependent atomic amplifier. We have achieved a maximum probe amplification of 7.5 dB with a visibility of 98.8% in the presence of ground state coherence. The amplification is shown to decrease sharply with increasing two-photon detuning. However, a nonzero amplification is present even with a large two-photon detuning of 15 MHz with reasonably high visibility of 66.8%. Our experimental results agree very well with our theoretical calculations.

Our experiment shows that for high amplification in a PDA, it is necessary to establish ground state coherence. However, for practical implementations of a PDA, we can sacrifice amplification for bandwidth. Thus one can make a judicious choice between amplification and bandwidth depending upon the application. This atom-based PDA can potentially serve as a very good interface for coherent conversion and amplification of quantum information generated in the microwave domain and converted to optical frequencies.

2. Experimental details

The hyperfine energy levels used in the experiment are $5^2S_{1/2}$, F = 2 ($|1\rangle$), $5^2S_{1/2}$, F = 3 ($|2\rangle$) and $5^2P_{1/2}$, F' = 3 ($|3\rangle$). An optical coupling field (ω_c) with Rabi frequency Ω_c connects the transition $5^2S_{1/2}$, F = 3 ($|2\rangle$) $\longrightarrow$ $5^2P_{1/2}$, F' = 3 ($|3\rangle$). A microwave field (ω_{RF}) at 3.0357 GHz, having a Rabi frequency Ω_{RF} induces a magnetic dipole transition between the states $5^2S_{1/2}$, F = 2 ($|1\rangle$) and $5^2S_{1/2}$, F = 3 ($|2\rangle$). The weak magnetic dipole transition is enhanced using a microwave cavity resonating at 3.0357 GHz frequency with a quality factor of 10000±1000. A probe field (ω_p) connects the states $|1\rangle$ and $|3\rangle$, with a Rabi frequency Ω_p. The microwave and the two coupling and probe optical fields connect the hyper-fine levels of the room temperature ^{85}Rb atoms in a cyclic configuration. This will be hereafter referred to as a Δ system shown in Fig. 1(a).

A schematic representation of our experimental setup is shown in Fig. 1(b). An ECDL has been used to derive the coupling beam, which enters a fiber coupled electro-optic modulator (EOM) driven by the microwave source to produce the probe field. The probe and coupling beams pass through a vapour cell kept inside the microwave cavity at room temperature. The cavity supports a standing wave at 3.0357 GHz and so the atoms inside the cavity are subjected to two optical and one microwave field. The optical fields after interaction emerge from the cavity and the probe field is separated from the coupling field by heterodyne detection. The amplitude of the probe field is analyzed using a spectrum analyzer. A digital phase shifter has been used to control the phase of the microwave field, which enters the cavity. The optical power of probe and coupling fields are kept constant at 33 μW and 166 μW respectively and the optical density of the sample is calculated to be 1.0. The power of optical fields are chosen for values where the gain is a maximum. The optical depth is fixed by the lowest detectable probe power by our high band-width detector.

The microwave cavity and the EOM are driven by the same source of microwave field, ensuring relative phase stability between all the three fields. Throughout the experiment, a three-photon resonance condition $\delta_3 = \delta_p - \delta_c - \delta_{RF} = 0$, is satisfied. Here δ_c, δ_p and δ_{RF} refer to the detunings of the coupling, probe and microwave fields from their respective transitions respectively (Fig. 1(a)). During all runs of our experiment, the value of δ_c is kept zero and the equality $\delta_p = \delta_{RF}$ is maintained. A change in δ_{RF} from its resonance thus enables selective

OSA CONTINUUM

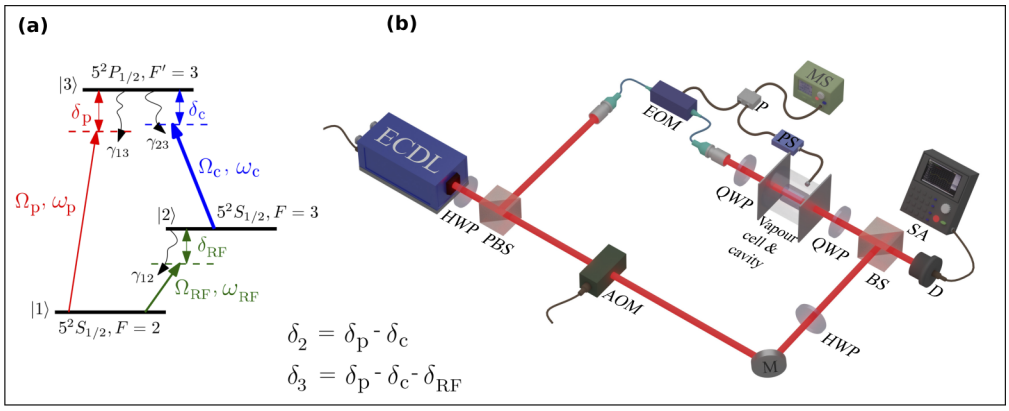

Fig. 1. (a) Energy level scheme. δ_2 and δ_3 are two photon and three photon detunings respectively.(b) Schematic of experimental set up. Here ECDL —External Cavity Diode Laser, HWP —half-wave plate, QWP —quarter wave-plate, PBS —polarizing beam-splitter, AOM —Acousto-optic modulator, M —Mirror, EOM —Electro-optic modulator, MS —Microwave source, P —Power splitter, PS —Phase shifter, D —Detector, SA —Spectrum analyzer.

breaking of two-photon resonance ($\delta_2 = \delta_p - \delta_c = 0$) while ensuring that the three-photon resonance condition remains satisfied.

We perform our experiment at a room temperature of 300 K. At this temperature we can still observe true amplification of the input seed probe field for appropriate values of input microwave and coupling powers.

3. Experimental observation

We observe amplification and de-amplification of the input probe beam as a result of nonlinear three-wave mixing interaction between the microwave and the two optical fields mediated by the Rb atoms. This is possible with the help of a microwave magnetic dipole transition, which allows a three-wave mixing phenomenon by breaking the centro-symmetry of the atom [19]. The amplification is dependent on the relative phase between all the three fields. This relative phase is defined as

$$\Delta\Phi(z) = \phi_{RF} + (k_p - k_c)z \tag{1}$$

where ϕ_{RF} is the phase of the microwave field and $k_p z$, $k_c z$ are the propagation phases of the probe and coupling field respectively [18]. Since the microwave field is inside a cavity, there are no propagation phases associated with it. The phases of probe and coupling field are taken to be the same as they are derived from the same source. When the relative phase $\Delta\Phi$ changes from 0 to π, the probe beam transits from a regime of amplification to a regime of de-amplification with a periodicity of 2π as reported in our previous study [18].

As a significant new step, in the current experiment, we investigate the gain (G) experienced by the probe field both in the presence and absence of two-photon induced ground state coherence. This is achieved by selectively detuning the probe field away from its resonance while maintaining the coupling field at its resonance. This breaks the two-photon resonance condition and renders $\delta_2 = \delta_p - \delta_c \neq 0$. Since our microwave source controls the EOM from which the probe laser is generated any microwave detuning δ_{RF} results in the same numerical value for the detuning δ_p of the probe laser. Thus a selective breaking of two-photon resonance is achieved while simultaneously maintaining the three-photon resonance necessary for efficient nonlinear wave

OSA CONTINUUM

mixing. The effect of this selective breaking of ground-state coherence on probe amplification is shown in Fig. 2.

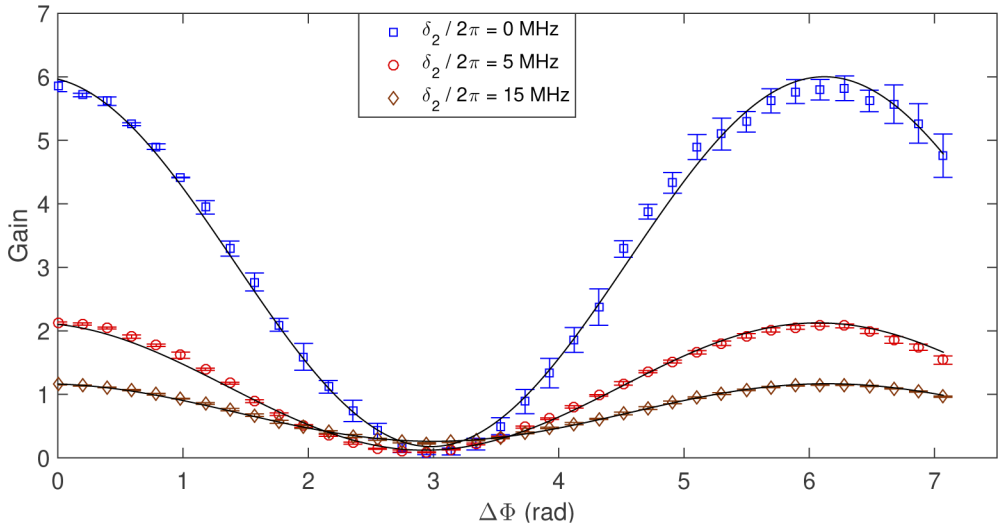

Fig. 2. Probe gain vs $\Delta\Phi$ for different values of δ_2 at microwave intensity 1.03 mW/cm^2. The continuous line is the theoretical fit.

In this plot, we have shown the variation of gain (G) of the probe field as a function of relative phase difference ($\Delta\Phi$) at different two-photon detunings δ_2. Here the gain G is calculated as the ratio of the transmitted probe power at a particular δ_2 to that at far-off-resonance where both the optical fields are away from their respective resonance by more than 1 GHz.

The maximum and minimum gain are defined as the highest amplification and de-amplification respectively, which is observed in the probe field. As can be seen in this figure, for $\delta_2 \neq 0$, the maximum gain decreases. Nevertheless, since $\delta_3 = 0$ and since our system is phase dependent,

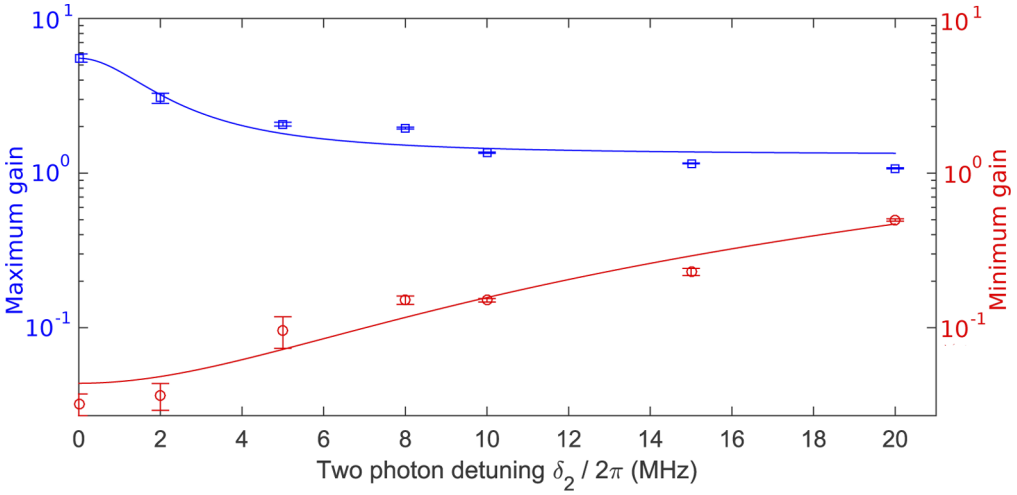

Fig. 3. Maximum and minimum gain vs δ_2 in log scale for microwave intensity of 1.03 mW/cm^2. Blue squares and red circles are experimental data points for maximum and minimum gain respectively. The continuous lines are theoretical fit.

OSA CONTINUUM

we can see that even at non-zero δ_2 we achieve phase dependent amplification (G>1) and de-amplification (G<1).

The variation of maximum gain and minimum gain as a function of δ_2 is plotted in Fig. 3. As can be seen from the plot the nonlinear wave mixing is highly efficient and coherently adds to the input probe resulting in maximum amplification of the probe in the presence of ground state coherence ($\delta_2 = 0$). As δ_2 increases, the maximum gain asymptotically reaches unity reflecting no gain. In a symmetric fashion, the minimum gain increases from its lowest value as δ_2 increases and also seen to tend to unity at large δ_2 values. The full width at half maximum (FWHM) of the amplification is found to be 5 MHz. A single data point represents an average of 150 data points. The error bars denote the statistical standard deviation in our data sets.

4. Analysis of the experimental results

In order to understand our experimental results we have done an analytical calculation which captures the probe response in our Δ system. We derive the interaction Hamiltonian of our Δ system under rotating wave approximation. We transform the Hamiltonian using unitary transformation $\hat{\mathrm{U}}(t) = |1\rangle\langle 1| + e^{i((\omega_\mathrm{p}-\omega_\mathrm{c})t-(k_\mathrm{p}-k_\mathrm{c})z+\phi_\mathrm{p}-\phi_\mathrm{c})}|2\rangle\langle 2| + e^{i(\omega_\mathrm{p}t-k_\mathrm{p}z+\phi_\mathrm{p})}|3\rangle\langle 3|$ and obtain a time independent Hamiltonian under three-photon resonance condition, with ground state $|1\rangle$ as the reference level.

$$\begin{aligned}\hat{H}(\boldsymbol{r},\boldsymbol{v}) = &-\Delta_\mathrm{p}(\boldsymbol{v})|3\rangle\langle 3| - (\Delta_\mathrm{p}(\boldsymbol{v}) - \Delta_\mathrm{c}(\boldsymbol{v}))|2\rangle\langle 2| - \frac{\Omega_\mathrm{p}(\boldsymbol{r})}{2}|3\rangle\langle 1| \\ &- \frac{\Omega_\mathrm{c}(\boldsymbol{r})}{2}|3\rangle\langle 2| - \frac{\Omega_\mathrm{RF}(\boldsymbol{r})e^{-i\Delta\Phi}}{2}|2\rangle\langle 1| + \mathrm{H.C.},\end{aligned} \tag{2}$$

with H.C. denoting Hermitian conjugate, $\Delta\Phi$ is the relative phase between all the fields given in Eq. (1) and $\hbar$ is taken to be 1. The Doppler-shifted detunings of the probe and coupling fields, as seen by an atom moving with velocity $\boldsymbol{v}$ are given by $\Delta_\mathrm{p}(\boldsymbol{v}) := \delta_\mathrm{p} - \boldsymbol{k}_\mathrm{p}\cdot\boldsymbol{v}$ and $\Delta_\mathrm{c}(\boldsymbol{v}) := \delta_\mathrm{c} - \boldsymbol{k}_\mathrm{c}\cdot\boldsymbol{v}$. Here $\Omega_\mathrm{p}(\boldsymbol{r}) = \boldsymbol{d}_{13}\cdot\boldsymbol{E}_\mathrm{p}(\boldsymbol{r})$, $\Omega_\mathrm{c}(\boldsymbol{r}) = \boldsymbol{d}_{23}\cdot\boldsymbol{E}_\mathrm{c}(\boldsymbol{r})$ and $\Omega_\mathrm{RF}(\boldsymbol{r}) = \boldsymbol{\mu_{12}}\cdot\boldsymbol{B}_\mathrm{RF}(\boldsymbol{r})$ are the Rabi frequencies. $\boldsymbol{d}_\mathrm{ij}$ and $\boldsymbol{\mu}_\mathrm{ij}$ are the electric and magnetic dipole matrix elements respectively. All optical fields are taken to be propagating along the z direction. The symbols $\boldsymbol{E}_\mathrm{p}$,$\boldsymbol{E}_\mathrm{c}$ are the electric fields of the probe and coupling optical fields respectively. $\boldsymbol{B}_\mathrm{RF}$ is the microwave magnetic field flux density. The dynamical evolution of rotated density matrix $\hat{\sigma}(t) = \hat{\mathrm{U}}(t)\hat{\rho}(t)\hat{\mathrm{U}}^\dagger(t)$, is given by the master equation [20]

$$\frac{\partial\hat{\sigma}(\boldsymbol{v},z,t)}{\partial t} = -i[\hat{H}(\boldsymbol{v},z),\hat{\sigma}(\boldsymbol{v},z,t)] + \sum_{k=1}^{5}\mathcal{L}(\hat{a}_k)\hat{\sigma}(\boldsymbol{v},z,t) \tag{3}$$

with $\mathcal{L}(\hat{a}_k)$ the Lindblad superoperator

$$\mathcal{L}(\hat{a})\hat{\sigma}(\boldsymbol{v},z,t) = \hat{a}\hat{\sigma}(\boldsymbol{v},z,t)\hat{a}^\dagger - \frac{1}{2}\{\hat{\sigma}(\boldsymbol{v},z,t),\hat{a}^\dagger\hat{a}\} \tag{4}$$

acting on operators $\hat{a}_1 = \sqrt{(\bar{n}+1)\gamma_{12}}|1\rangle\langle 2|$, $\hat{a}_2 = \sqrt{\bar{n}\gamma_{12}}|2\rangle\langle 1|$, $\hat{a}_3 = \sqrt{\gamma_{13}}|1\rangle\langle 3|$, $\hat{a}_4 = \sqrt{\gamma_{23}}|2\rangle\langle 3|$ and $\hat{a}_5 = \sqrt{\gamma_c}(|1\rangle\langle 1| - |2\rangle\langle 2|)$ with γ_{12} and $\gamma_{23} = \gamma_{13}$ representing natural linewidth of levels $|2\rangle$ and $|3\rangle$ respectively, $\bar{n}$ is the average number of thermal photons and γ_c being the phenomenological decay constant modeling the finite quality factor of our microwave cavity. In the limit of weak probe and microwave fields, Ω_p<$\Omega_\mathrm{RF} \ll \Omega_\mathrm{c}$ we can assume $\sigma_{11} \approx 1$. Solving Eq. (3) for σ_{31} at

OSA CONTINUUM

steady state we obtain

$$\sigma_{31}(\boldsymbol{v},z)=\frac{2i\Gamma_2\Gamma_3\Omega_{\rm p}(z)}{4\Gamma_1\Gamma_2\Gamma_3+\Gamma_3|\Omega_{\rm c}(z)|^2+\Gamma_2|\Omega_{\rm RF}(z)|^2}-\frac{\Gamma_3\Omega_{\rm c}(z)\Omega_{\rm RF}(z)e^{-i\Delta\Phi}}{4\Gamma_1\Gamma_2\Gamma_3+\Gamma_3|\Omega_{\rm c}(z)|^2+\Gamma_2|\Omega_{\rm RF}(z)|^2} \tag{5}$$

Here

$$\begin{aligned}\Gamma_1&=\frac{\gamma_{13}}{2}+\frac{\gamma_{23}}{2}+\frac{\bar{n}\gamma_{12}}{2}+\frac{\gamma_c}{2}-i\Delta_{\rm p},\quad \Gamma_2=(\bar{n}+\frac{1}{2})\gamma_{12}-i(\delta_2-\boldsymbol{k}_{\rm p}\cdot\boldsymbol{v}+\boldsymbol{k}_{\rm c}\cdot\boldsymbol{v}),\\ \Gamma_3&=\frac{\gamma_{13}}{2}+\frac{\gamma_{23}}{2}+(\frac{\bar{n}+1}{2})\gamma_{12}+\frac{\gamma_c}{2}-i\Delta_{\rm c}\end{aligned} \tag{6}$$

In Eq. (5) the coefficient of $\Omega_{\rm p}$ in the first term is proportional to the linear susceptibility of the probe field and the coefficient of $\Omega_{\rm c}\Omega_{\rm RF}$ in the second term is proportional to the hybrid second order susceptibility of probe field. This nonlinear susceptibility results from a combined magnetic and an electric dipole transition induced by microwave field and optical coupling field respectively resulting in a new optical probe field generation.

Using the slowly-varying envelope approximation, we calculate the propagation equation for the probe field inside our nonlinear medium as given below.

$$\frac{\partial\Omega_{\rm p}}{\partial z}=i\eta_{\rm p}\sigma_{31}, \tag{7}$$

where $\eta_{\rm p}=(\boldsymbol{d}_{13}^2\omega_{\rm p}N/2\epsilon_0c\hbar)$ is the coupling constant for the probe field and N is the number density of atoms. The propagation effect of the microwave field is not taken into account due to the fact that the ratio $\eta_{\rm RF}/\eta_{\rm p}=(\omega_{\rm RF}/\omega_{\rm p})\alpha^2$, where $\alpha\approx 1/137$ is the fine structure constant. This results in $\eta_{\rm RF}\ll\eta_{\rm p}$ and the spatial variation of microwave intensity is thus ignored. We therefore maintain $\Omega_{\rm RF}(z)\equiv\Omega_{\rm RF}(0)$ in our theoretical analysis. In addition, the undepleted pump approximation is valid for the coupling field in our system. This fact is incorporated by taking $\Omega_{\rm c}(z)\equiv\Omega_{\rm c}(0)$. We thus solve for Eq. (7) in spatially uniform coupling and microwave fields, resulting in the following solution for the probe field.

$$\Omega_{\rm p}(l)=\Omega_{\rm p}(0)e^{-\beta l}+\frac{i\Omega_{\rm c}(0)\Omega_{\rm RF}(0)e^{-i\Delta\Phi}}{2\Gamma_2}(e^{-\beta l}-1) \tag{8}$$

where $\beta=(2\eta_{\rm p}\Gamma_2\Gamma_3)/(4\Gamma_1\Gamma_2\Gamma_3+\Gamma_3|\Omega_{\rm c}(0)|^2+\Gamma_2|\Omega_{\rm RF}(0)|^2)$. It is to be noted that β is a complex number. The total probe amplitude at the end of the cell with length l is given by Eq. (8). Using a Maxwell-Boltzmann velocity averaged Eq. (8) at a temperature of 300 K in accordance with our experiment we see that our experimental data shown in Fig. 2 and Fig. 3 match very well with our theoretical analysis. The Eq. (8) also captures the important physical effect of interference present in our system. This interference effect is explained below.

The first term in Eq. (8) represents phase changes and losses suffered by the input probe field due to linear susceptibility and the second term represents similar changes experienced by the generated probe field [19]. The input probe and the generated probe field amplitudes interfere constructively or destructively for appropriate values of $\Delta\Phi$ which results in either amplification or de-amplification of the probe field respectively. At two-photon resonance ($\delta_2=0$), the input probe field and generated probe field will propagate with minimal losses due to EIT effect. In addition, probe field generation is most efficient at $\delta_2=0$ resulting in a maximum gain for the probe. When the ground state coherence condition is not satisfied ($\delta_2\neq 0$), the input probe field experiences linear absorption due to absence of EIT and also the probe generation reduces as $1/\delta_2$ due to which the maximum gain decreases. The de-amplification effect is due to destructive interference and therefore the second term acquires a negative sign during de-amplification resulting in an increase in the minimum gain value. As can be seen from both the experimental

OSA CONTINUUM

data points and our theoretical fit in Fig. 3, the maximum gain and minimum gain curves reflect this symmetry.

Visibility is an important parameter for interference. In analogy with the interference of two fields arising from the two slits of a double-slit experiment, we identify the generated probe and the seed probe to be the two interfering fields. Extending this analogy, we can associate the maximum gain and minimum gain in our experiment to the bright and dark fringes of the interference pattern respectively. Using this comparison, the visibility at any given δ_2 is defined as the ratio between the difference of maximum gain and minimum gain to their sum. From Fig. 3, it is clear that the maximum gain and the minimum gain asymptotically tend to unity for high two photon detunings as explained earlier. For $\delta_2 = 0$, both the two-photon and three-photon resonance conditions are satisfied which maximises the ground state coherence assisted generation of the probe. Hence visibility is maximum for this value and under ideal conditions will be unity. On the other end, for large non-zero values of δ_2, visibility will be at its lowest due to the negligible generation of the probe field and will tend to zero. This behaviour is experimentally observed, as seen in Fig. 4.

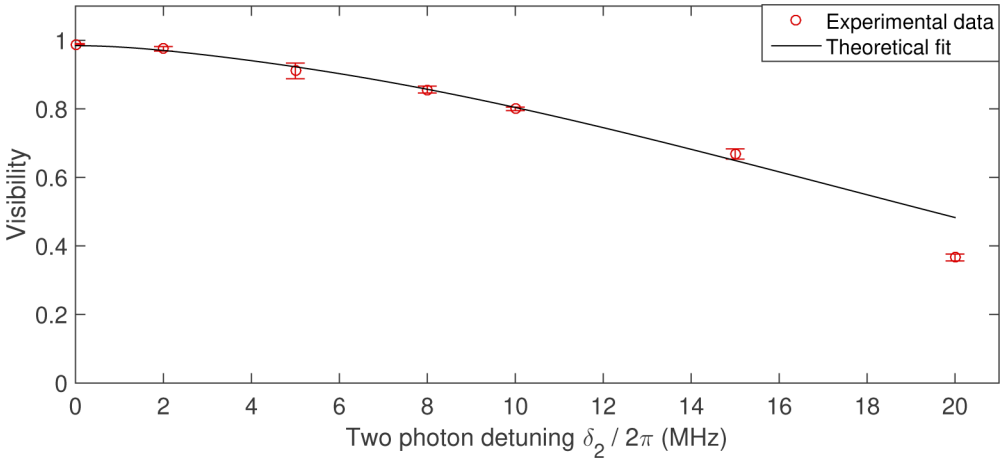

Fig. 4. Visibility vs δ_2 for microwave intensity of 1.03 mW/cm^2.

A large visibility value in our experiment indicates that the generated and input probe fields have similar amplitudes. This is desirable in optical switches and digital communication [1,2]. In our experiment, we obtain high visibility of 98.8% at $\delta_2/2\pi = 0$ and visibility of 66.8% at $\delta_2/2\pi = 15$ MHz as shown in Fig. 4. It is important to note from Fig. 4 that faithful transmission of signals is possible with very little amplification for two-photon detunings as large as 20 MHz with visibility close to 37 % which is $1/e$ value of the visibility curve. Thus our PDA gives us the freedom to choose amplification over bandwidth and vice-versa depending upon the application.

In order to understand the dependence of visibility on microwave intensity, we have plotted the variation of visibility with microwave intensity in Fig. 5 for $\delta_2/2\pi = 5$ MHz. Visibility increases as microwave intensity increases and shows saturation beyond 0.4 mW/cm^2. This is because, as microwave intensity increases, the probe generation will increase up to a point where absorption associated with nonlinearity will saturate any further increase [19]. This in-turn leads to a saturation in the maximum gain and the minimum gain and consequently the visibility.

We have measured the variation of signal to noise ratio (SNR) of the optical output probe field for different values of two photon detuning to understand the signal quality of the output signal. As expected the SNR is found to be decreasing with increasing δ_2 as shown in Fig. 6. However this decrease is very less. From a large SNR of 90 dB at resonance for a $\delta_2/2\pi = 0$, the SNR

OSA CONTINUUM

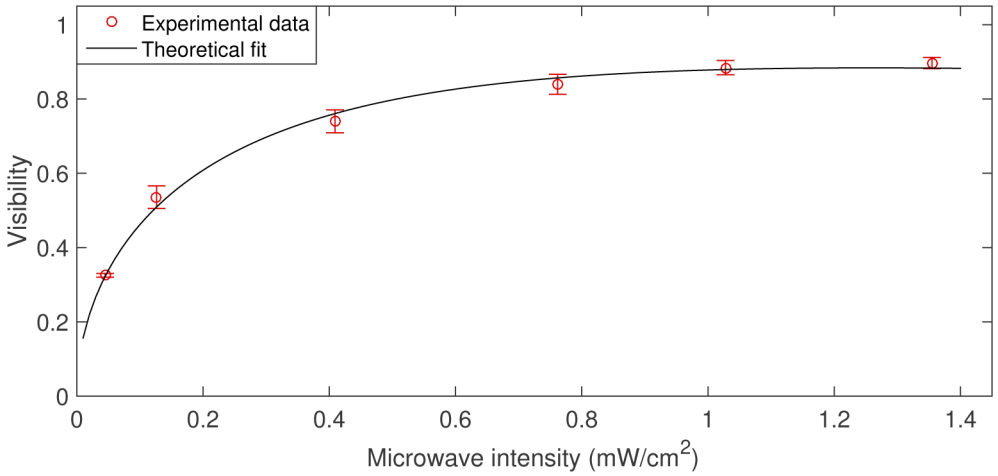

Fig. 5. Visibility vs microwave intensity for $\delta_2/2\pi = 5$ MHz.

decreases only to 71 dB even at a $\delta_2/2\pi = 20$ MHz. This signifies that our atomic PDA has a large data capacity for communication purposes even at a bandwidth of 20 MHz.

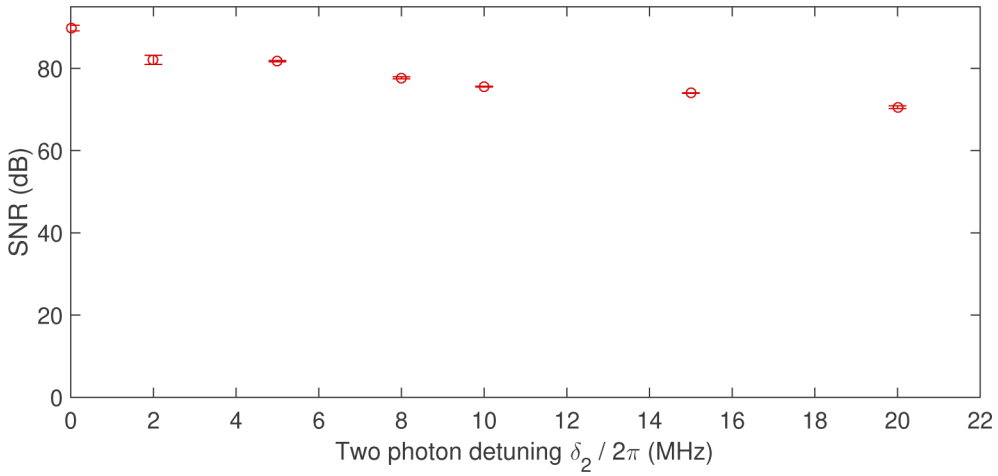

Fig. 6. SNR of the optical output probe field vs δ_2 for microwave intensity of 1.03 mW/cm^2.

5. Conclusion

We experimentally investigate the role of microwave controlled ground state coherence on a phase dependent optical amplifier. We show that the highest amplification is achieved only in the presence of ground state coherence. Through our experiment and subsequent analysis, we show that amplification is due to an interference process resulting in a maximum probe amplification of 7.5 dB with visibility of 98.8%. We also obtain a non-zero amplification with a visibility of 66.8% at a two-photon detuning of 15 MHz. The SNR of the output optical probe field is found to be high with values ranging from 90 dB at two-photon resonance to 70 dB at a bandwidth of 20 MHz. This enables us to make a judicious choice between amplification and bandwidth in accordance with our end application. We envisage that our atom-based hybrid optical amplifier

OSA CONTINUUM

will serve as a good interface for coherent transfer and amplification of classical and quantum microwave signals to optical frequencies.

Disclosures. The authors declare no conflicts of interest.

References

1. D. H. Meyer, K. C. Cox, F. K. Fatemi, and P. D. Kunz, "Digital communication with rydberg atoms and amplitude-modulated microwave fields," Appl. Phys. Lett. **112**(21), 211108 (2018).
2. C. L. Holloway, M. T. Simons, J. A. Gordon, and D. Novotny, "Detecting and receiving phase-modulated signals with a rydberg atom-based receiver," IEEE Antennas Wirel. Propag. Lett. **18**(9), 1853–1857 (2019).
3. A. Tretiakov, C. A. Potts, T. S. Lee, M. J. Thiessen, J. P. Davis, and L. J. LeBlanc, "Atomic microwave-to-optical signal transduction via magnetic-field coupling in a resonant microwave cavity," Appl. Phys. Lett. **116**(16), 164101 (2020).
4. Z.-L. Xiang, S. Ashhab, J. Q. You, and F. Nori, "Hybrid quantum circuits: Superconducting circuits interacting with other quantum systems," Rev. Mod. Phys. **85**(2), 623–653 (2013).
5. N. J. Lambert, A. Rueda, F. Sedlmeir, and H. G. L. Schwefel, "Coherent conversion between microwave and optical photons–an overview of physical implementations," Adv. Quantum Technol. **3**(1), 1900077 (2020).
6. R. W. Boyd, *Nonlinear Optics, Third Edition* (Academic, 2008), 3rd ed.
7. K.-J. Boller, A. Imamoğlu, and S. E. Harris, "Observation of electromagnetically induced transparency," Phys. Rev. Lett. **66**(20), 2593–2596 (1991).
8. J. E. Field, K. H. Hahn, and S. E. Harris, "Observation of electromagnetically induced transparency in collisionally broadened lead vapor," Phys. Rev. Lett. **67**(22), 3062–3065 (1991).
9. G. Alzetta, A. Gozzini, L. Moi, and G. Orriols, "An experimental method for the observation of r.f. transitions and laser beat resonances in oriented na vapour," Il Nuovo Cimento B (1971-1996) **36**(1), 5–20 (1976).
10. E. Arimondo and G. Orriols, "Nonabsorbing atomic coherences by coherent two-photon transitions in a three-level optical pumping," Lett. al Nuovo Cimento (1971-1985) **17**(10), 333–338 (1976).
11. H. R. Gray, R. M. Whitley, and C. R. Stroud, "Coherent trapping of atomic populations," Opt. Lett. **3**(6), 218–220 (1978).
12. M. Fleischhauer, A. Imamoglu, and J. P. Marangos, "Electromagnetically induced transparency: Optics in coherent media," Rev. Mod. Phys. **77**(2), 633–673 (2005).
13. S. E. Harris, J. E. Field, and A. Imamoğlu, "Nonlinear optical processes using electromagnetically induced transparency," Phys. Rev. Lett. **64**(10), 1107–1110 (1990).
14. M. D. Lukin, P. R. Hemmer, M. Löffler, and M. O. Scully, "Resonant enhancement of parametric processes via radiative interference and induced coherence," Phys. Rev. Lett. **81**(13), 2675–2678 (1998).
15. F. Wen, H. Zheng, X. Xue, H. Chen, J. Song, and Y. Zhang, "Electromagnetically induced transparency-assisted four-wave mixing process in the diamond-type four-level atomic system," Opt. Mater. **37**, 724–726 (2014).
16. C. Ye and J. Zhang, "Electromagnetically induced transparency-like effect in the degenerate triple-resonant optical parametric amplifier," Opt. Lett. **33**(16), 1911–1913 (2008).
17. K. Li, Y. Cai, W. Li, H. Fan, S. Ning, S. Zhang, and Y. Zhang, "All-optical wavelength division multiplexing amplifier based on vacuum induced nonreciprocal bistability in six-wave mixing process with a ring cavity," Results Phys. **16**, 102822 (2020).
18. A. Karigowda, A. K. V P. K. Nayak, S. Sudha, B. C. Sanders, F. Bretenaker, and A. Narayanan, "Phase-sensitive amplification of an optical field using microwaves," Opt. Express **27**(22), 32111–32121 (2019).
19. K. V. Adwaith, A. Karigowda, C. Manwatkar, F. Bretenaker, and A. Narayanan, "Coherent microwave-to-optical conversion by three-wave mixing in room temperature atomic system," Opt. Lett. **44**(1), 33–36 (2019).
20. M. Manjappa, S. S. Undurti, A. Karigowda, A. Narayanan, and B. C. Sanders, "Effects of temperature and ground-state coherence decay on enhancement and amplification in a Δ atomic system," Phys. Rev. A **90**(4), 043859 (2014).